Selection of Brownian particles

Luc P. Faucheux and Albert Libchaber*
Rockefeller University, 1230 York Av., NY NY 10021.

Abstract

A macroscopic drift of Brownian particles (1.5 and 2.5 microns diameter silica spheres in water) is induced by switching on and off a spatially periodic asymmetric potential. It is defined by an AC voltage, applied between asymmetrically shaped metallic electrodes deposited on a glass plate. The induced drift is function of the particle diffusion coefficient, one can thus select particles according to their size.

In the absence of external forces, Brownian particles do not experience any macroscopic drift. In a similar way, a spatially periodic external potential, asymmetric or not, does not induce large scale motion as the associated large scale gradient (force) is zero. However, a time modulation between the two regimes (free diffusion, applied potential) induces macroscopic drifts of Brownian particles, when the potential is asymmetric [1, 2]. Other mechanisms of motion have also been proposed [3, 4]. The principle is the following: the field traps the particles in the potential minima (see Fig. 1). They freely diffuse when the field is off. Switching the field on again after a modulation time τ_{mod}, the particles follow the local gradient of potential and get trapped in the corresponding minimum. Given the asymmetry of the potential, the particles average diffusion time over the right barrier is shorter than over the left one, thus trapping into the right well is preferred. Repeating this process induces a macroscopic drift of particles, from left to right (Fig. 1). The induced drift is function of the diffusion coefficient of the particles and the modulation time: for small τ_{mod}, the drift is zero, the particles do not have enough time to diffuse; for large τ_{mod}, the drift is also zero, they have enough time to diffuse equally on both sides. In between, the induced drift exhibits a maximum, related to stochastic resonance [5].

Such a system can be used in principle [6] to separate particles

of different sizes (hence different diffusion coefficients). One way to measure the induced drift experimentally is to create the desired potential with optical tweezers [7]. The experiment confirmed quantitatively the theoretical predictions. However, only one particle can be trapped at a time. Another way which allows more than one particle to be trapped, is to build a dielectrophoretic cell by depositing metallic electrodes on a glass plate: the potential is then created electrically by applying an AC field between the electrodes, attracting dielectric particles. The Brownian particles used are micron sized spheres easily visualized under the microscope. This simple experimental setup was first proposed by J. Rousselet and co-workers [8]. We extend here their experimental results and show that particle separation is feasible.

This paper is divided as follows: we first describe the sample preparation and the experimental setup. We then present the results and a simple theoretical model. Finally, we discuss particles separation. Frequency dependence of the forcing field is described in the Appendix.

Experimental setup

The cell is bounded by a glass bottom plate and a coverslip on top of it, sealed laterally. The bottom plate of the cell is obtained in the following way: a thin layer of metal (300 Å Chromium, 1500 Å Gold) is first deposited by lithography techniques [9] onto a microscope slide following the pattern shown in Fig. 2. It consists of a network of interdigited fingers, each finger presenting a "Christmas tree" structure. We connect the electrodes to a function generator [10] via electrical wires, held onto the bottom plate with fast epoxy. A silver epoxy [11] junction between the wires and the electrodes ensures electrical conduction. We then spincoat [12] on top of the metal electrodes a glass film [13], a dielectric insulator that prevents electrical contact leading to irreversible sticking between the particles and the electrodes. It also creates a flat surface for the particles on which they can freely diffuse. Finally, it acts as a passivation layer for the electrodes and prevents fluid flow in the cell due to charge injection instabilities [14]. This layer has to be thick enough to prevent electrical contact, but thin enough so that the field is not completely screened in the sample. The optimal thickness is of order 1 micron (8 drops of Silicafilm deposited every

ten seconds, spincoat at 3 krpm).

Commercial suspensions of 1.5 and 2.5 microns diameter silica spheres [15] are diluted in pure water down to volume fractions of order 10^{-2}. Mylar sheets, 50 microns thickness, are cut and used as spacers between the bottom plate and a coverslip. Glassware are cleaned and then dried using a Nitrogen ionizing gun [16]. The cells are then filled with a suspension of spheres and sealed with nail polish [17] to avoid any convective flow. Nail polish was chosen instead of five minutes epoxy [18], wax, Torr seal [19] and optically cured adhesive [20] because of its ionic stability: the response of the particles to an applied electrical field would not change over periods of two to three hours (see Appendix). The gravitational field g keeps the particles close to the bottom plate. An estimate of this sedimentation effect is the Boltzmann length scale $L = \frac{k_B T}{\Delta m g}$, where Δm is the relative mass of the particle. L, around 0.1 microns, is the average vertical excursions of the particles caused by thermal fluctuations. Since L is smaller than the particle radius r, the particles are confined almost at contact with the bottom plate, diffusing in two dimensions. The cell is placed on the stage of an inverted microscope [21] and the particles are observed under bright light transmission [22]. They appear dark on a clear background.

Experimental procedure

We now modulate in time an AC electrical field, 100 kHz, 1V across the electrodes. Following the midline between two fingers in Fig. 2b, the field intensity is periodic asymmetric, maximum between two finger tips (minimum distance between the electrodes, 5 microns) and minimum between two dips (maximum distance, 40 microns). In the 100 kHz frequency range, the particles response is driven by dipolar effects, characterized by the value of the refractive index. We buffer the water with NaCl ions (10^{-3} M) so that the refractive index of the particles is smaller that the one of the electrolyte solution: the particles are attracted to the regions of minimum intensity (Fig. 3, τ=0 s). The attractive potential experienced by the particles is periodic asymmetric, characterized by the forward and backward length scales λ_f and λ_b (Fig. 3, τ=0). The potential depth is such that the particles never escape from the trap.

This first step is the localization step: the single particle probability density along the midline between the electrodes is sharply peaked around the potential minimum (Fig. 3, τ=0).

Diffusion step. The electrical field is switched off: the particles are free to diffuse in two dimensions above the bottom plate (Fig. 3, τ=95 s). The electrodes (dark regions in Fig. 3) do not constitute an obstacle. The solid line in Fig. 3 separates particle originating from two adjacent potential minima. The probability density for one particle spreads as a Gaussian (Fig. 3, $\tau < \tau_{mod}$).

After a time τ_{mod} the electrical field is switched back on: the particles get localized again in the potential minima. The potential profile is asymmetric ($\lambda_f < \lambda_b$), thus P_f, trapping probability into the forward well, is larger than P_b, trapping probability into the backwards well: $P_f > P_b$. In Fig. 3, out of the 74 particles from the middle well, ten particles advance to the right after a time τ=98 s ($P_f \approx 10/74$), and none to the left well ($P_b \approx 0$).

Theoretical model

P_f and P_b can be theoretically estimated using a single particle, one dimensional model. They are equal to the area under the Gaussian probability density shown in Fig. 3, $\tau < \tau_{mod}$. Because the particle does not have enough time to diffuse by more than 1 well, we normalize and integrate the Gaussian from $-\infty$ to $+\infty$. The resulting error function is approximated as [8]:

$$P_f = \frac{1}{2}\mathrm{Erfc}\left[\sqrt{\frac{\tau_f}{2\tau_{mod}}}\right] \approx \frac{1}{2}\exp\left[\frac{-\tau_f}{\tau_{mod}}\right], \qquad (1)$$

and $P_b \approx \frac{1}{2}\exp\left[\frac{-\tau_b}{\tau_{mod}}\right]$ where the characteristic diffusive times τ_f and τ_b over the lengths λ_f and λ_b are:

$$\tau_f = \left(\lambda_f^2/2D\right) = \left(\lambda_f^2 \frac{6\pi\eta r}{2k_B T}\right), \qquad (2)$$

and $\tau_b = \left(\lambda_b^2/2D\right) = \left(\lambda_b^2 \frac{6\pi\eta r}{2k_B T}\right)$. D is the Stokes-Einstein diffusion coefficient [23], η the bulk viscosity of water and r the particle radius.

Results and discussion

Accumulating data over 20 to 40 different traps (about 1500 particles) for a given modulation time τ_{mod}, we measure the probability P_f and P_b for two different particle diameters. Experimental points in Fig. 4 correspond to runs with monodispersed (1.5 and 2.5 microns diameter alone) and mixed (1.5 and 2.5 microns together) particle solutions. The vertical error bars represent the statistical uncertainties. The main source of errors in the experiment is caused by particles diffusing over the electrodes where visualization is no longer possible. The two forward diffusive probabilities P_f start from zero for small modulation time (the particles do not have time to diffuse over to the next well) and saturates for large modulation times to a value close to 1/2. Larger particles (2.5 microns) have a smaller diffusion coefficient: their diffusive probability P_f is thus smaller. Particle separation is possible: for τ_{mod} around 100 seconds, the two forward diffusive probabilities differ by an order of magnitude. P_b is measured to be zero throughout the experiments for both particle sizes.

We now analyze the results. The solid lines in Fig. 4 are a fit of eq. 1 to the experimental points. The fits yields $\tau_{f(1.5)} \approx 130\,s$ for 1.5 microns and $\tau_{f(2.5)} \approx 380\,s$ for 2.5 microns. These are the only directly measured quantities.

In principle the lengths λ_f and λ_b are geometrically defined. In fact, they are particle dependent. From eq. 2 we obtain a forward diffusive length $\lambda_{f(1.5)} \approx 8.7$ microns and $\lambda_{f(2.5)} \approx 11.5$ microns for 1.5 and 2.5 microns diameter particles respectively: the potential profile is function of the particle diameters.

The agreement between the experimental curves and eq. 1 is surprising. The particle diffusion is two dimensional and hindered by the presence of other particles. This crowding effect is responsible for the fact that P_b=0 for the whole range of τ_{mod}: particles can not

diffuse backward because of the steric repulsion of the others coming from the left well. This is not taken into account in the one dimensional, single particle model. Deviations of the diffusion coefficient from the Stokes Einstein law due to hydrodynamic interactions with other particles [24, 25], and with the bottom plate [26] should also be taken into account. Another complication is the fact that the potential profile is function of the particle diameter in a non trivial way ($\lambda_{f(1.5)} \neq \lambda_{f(2.5)}$). Finally, we neglected any interactions between particles caused by the alternating electrical field [27].

In the work of Rousselet the particles were trapped at the electrodes tips. This seems to affect the value at saturation of P_f (see Appendix). Also, since they use light polystyrene spheres (large vertical excursions), the particles diffusion is three dimensional. In our case, the beads are localized near the bottom plate, the diffusion is purely two dimensional. Finally we extended the range in modulation time by a factor 2 (from 150 seconds to 300 seconds), allowing us to observe the saturation of P_f for large τ_{mod}.

In conclusion, by modulating in time a periodic asymmetric potential, we induce macroscopic drift of Brownian particles. The drift is function of the diffusion coefficient, thus particles of different sizes can be selected. A one dimensional, single particle, model agrees qualitatively with our measurements. A complete theory must include the effect of hydrodynamic interactions, field profile inside the cell and frequency dependence of the potential.

Appendix: Frequency effects

We discuss here the frequency dependence of the potential profile for 1.5 microns diameter particles. Changing the field amplitude only accentuates but does not change qualitatively the particles response. Water electrolysis occurs for amplitude above 5 V (field amplitude of order 10^6 $V.m^{-1}$).

At low frequencies (below 6 Hz), the particle motion is driven by the charges: the particles move back and forth between the two electrodes at the field frequency.

Between 10 Hz and 100 Hz, the field oscillates too fast for the charged particles to respond. A convective roll close to the electrodes starts to appear at a frequency of order 1 Hz. The position of this convective roll moves from the triangle dips to the triangle tips as the frequency increases (Fig. 5, 10 Hz, 30 Hz, 50 Hz). The width of the roll also spreads as the frequency increases.

Between 100 Hz and 100 kHz, the particles disappear from the field of view: they lay on top of the electrodes and cannot be visualized (Fig. 5, 10 kHz).

Around 100 kHz, the particles are trapped between the electrodes tips (maximum field intensity). This regime only appears in pure water solution when sealing the cell with five minute epoxy. It disappears over time scales of order 20 minutes. We never observe this regime when buffering the solution (10^{-3} M NaCl) or sealing the cell with nail polish.

Above 200 kHz, the particles are trapped between the electrodes dips (minimum field intensity). The width of this "banana" decreases with increasing frequency (Fig. 5, 200 kHz and 500 kHz). This regime is observed up to 60 MHz, the maximum frequency tested.

Can we understand in simple terms this zoology of behaviors? The problem is complicated: one has first to compute the field distribution inside the cell. This involves knowing the dispersion curve of the refractive index of the glass plate, the passivation layer on the bottom plate and the electrolyte. Once the field profile inside the cell is known, one must find where the particles are trapped: when the particles refractive index is larger than the electrolyte one, the particles are attracted in the regions of maximum field intensity. If not, they are attracted in the regions of minimum field intensity.

In the work of Rousselet et al. [8], the particles were trapped between the electrodes tips, like in Fig. 5, 100 kHz. This seems to affect the value at saturation of P_f, 0.9 instead of 0.5. Rousselet and coworkers, however, were using smaller particles made out of polystyrene with significant vertical excursion. We choose to work with silica particles because of their large density (2.1 instead of 1.05) so that they sediment to the bottom plate and do not diffuse in the vertical direction. For silica particles, the regime where the particles are trapped between the electrodes tips is, however, unstable against injections of ions into the solution: buffering the solution with ions increases the refractive index of the solution [28]. Once it is larger than the one of the particles, they switch from being between the tips (Fig. 5, 100 kHz) to being between the dips (like in Fig. 5, 200 kHz). In order to avoid time transient effects, we buffer the solution and trap the particles between the dips.

Below 6 Hz, the particle response is clearly determined by their charges. Between 6 Hz and 100 kHz, we think that the particles are attracted in the regions of maximum intensity, and their motion depends on the field configuration inside the cell. In particular, the frequency window where the particles lay on top of the electrodes (Fig. 5, 10 kHz) indicates that the field is concentrated just above the electrodes. Also the convective motion below 200 Hz indicates the presence of charge injections at the electrodes.

Acknowledgments

It is a pleasure to acknowledge Adam Simon who suffered with us on the early stages of this experiment. We thank Armand Ajdari and Jacques Prost for enlightening discussions. We would never have made it so far without the help and advice of Saleem Shaikh.

Figure captions

Figure 1: The periodic asymmetric potential. The double arrow points in the direction of the induced drift.

Figure 2: a) Experimental setup: the solid and striped regions are the metallic electrodes deposited onto a microscope slide. The solid electrodes are grounded, the striped ones are connected to a function generator.

b) Blow up of the interdigited fingers.

Figure 3: Visualization of the particles and corresponding time evolution of the probability density.

Localization step. The periodic dielectric potential is switched on (AC field 100 kHz, 1V). On the right (τ=0 s), experimental visualization: the electrodes are in black, the particles are trapped in the potential minima (banana shaped regions of minimum field intensity between the electrodes dips). On the left (τ=0), the one-dimensional, single particle model: the potential asymmetry is characterized by the two length scales λ_f and λ_b. The probability density is peaked at the potential minima .

Diffusion step, the field is switched off. On the right (τ=95 s), experimental visualization: the particles diffuse freely in two dimensions. The solid line separates particles coming from different potential wells. On the left ($\tau < \tau_{mod}$), the model: the probability density spreads out as a Gaussian along the electrodes axis.

Localization step, the field is switched back on. On the left (τ=98 s), experimental visualization: the particles are trapped again. In the picture 10 particles originating from the middle well have diffused over to the right. On the left ($\tau = \tau_{mod}$), the model: the particle is trapped to the right with a probability P_f, the integral of the probability density between λ_f and $+\infty$. It is trapped to the left well with a probability P_b, the integral of the probability density between $-\infty$ and $-\lambda_b$.

Figure 4: Experimental diffusive probability P_f for silica particles of diameter 1.5 (circles) and 2.5 microns (triangles). The vertical error bars represent the statistical uncertainty. The solid lines are a fit of eq. 1 to the experimental curves.

Figure 5: The response of 1.5 microns diameter particles for different electrical field frequencies. Field amplitude 1 V.

References

* Also at NEC Research Institute, 4 Independence Way, Princeton NJ 08544.

[1] A. Ajdari and J. Prost, *Proc. Natl. Acad. Sci. USA*, 1991, **88**, 4468.

[2] M. Magnasco, *Phys. Rev. Lett.*, 1993, **71**, 1477.

[3] R. Landauer andM. Büttiker, *Physica Scripta*, 1985, **T9**, 155.

[4] R. Landauer, *Physica A*, 1993, **194**, 551.

[5] H. A. Kramers, *Physica*, 1940, **7**, 284.

[6] A. Ajdari and J. Prost, *C. R. Acad. Sci. Paris*, 1992, **135**, 1635.

[7] L. P. Faucheux, L. S. Bourdieu, P. D. Kaplan, and A. J. Libchaber, *Phys. Rev. Lett.*, 1995, **74**, 1504.

[8] J. Rousselet, L. Salomé, A. Ajdari and J. Prost, *Nature*, 1994, **370**, 447.

[9] Thin Film Devices Inc., Anaheim, CA.

[10] Synthesizer model 3325A from Hewlett Packard Corp., Sunnyvale, CA.

[11] Colloidal silver liquid #12630 from Electron Microscopy Sciences, Ft Washington, PA.

[12] Photo resist spinner EC101DT from Headway Research Inc., Garland, TX.

[13] Silicafilm from Emulsitone Corp., Whippany, NJ.

[14] N. Felici, *C. r. hebd. Séanc. Acad. Sci. Paris*, 1971, **B 273**, 1004.

[15] Bangs Laboratories Inc., Carmel, IN.

[16] Topgun from Simco Inc., Hatfield, PA.

[17] Nail enamel hypo-allergenic "soft spice" from Almay Inc., NY.

[18] Fast epoxy from Devcon Corp., Danvers, MA.

[19] low vapor pressure resin from Varian Ass., Lexington, MA.

[20] Ultra violet curing optical adhesive from Norland Products Inc., New Brunswick, NJ.

[21] IMT-2 from Olympus Inc., Lake Success, CA.

[22] ULWD CD Plan 40 PL from Olympus Inc., Lake Success, CA.

[23] A. Einstein, *Ann. d. Phy. (4)*, 1906, **19**, 371.

[24] G. K. Batchelor, *J. Fluid Mech.*, 1976, **74**, 1.

[25] W. B. Russel, *Ann. Rev. Fluid Mech.*, 1981, **13**, 425.

[26] L. P. Faucheux and A. J. Libchaber, *Phys. Rev. E*,1994, **49**, 5158.

[27] Q. H. Wei, X. Y. Lei, C. H. Zhou, and N. B. Ming, *Phys. Rev. E*, 1995, **51**, 1586.

[28] R. P. Feynman, R. B. Leighton and M. Sands, in *The Feynman Lectures on Physics*, ed. Addison-Wesley, Readings, MA, 1964, section 32-5.

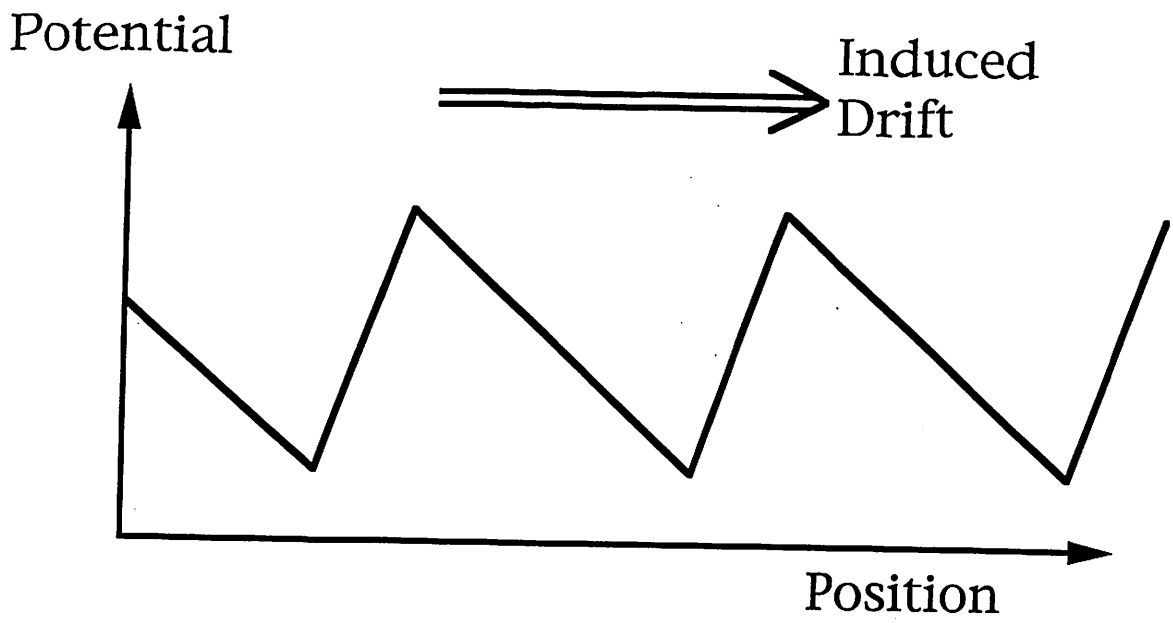

Faucheux and Libchaber

figure 1

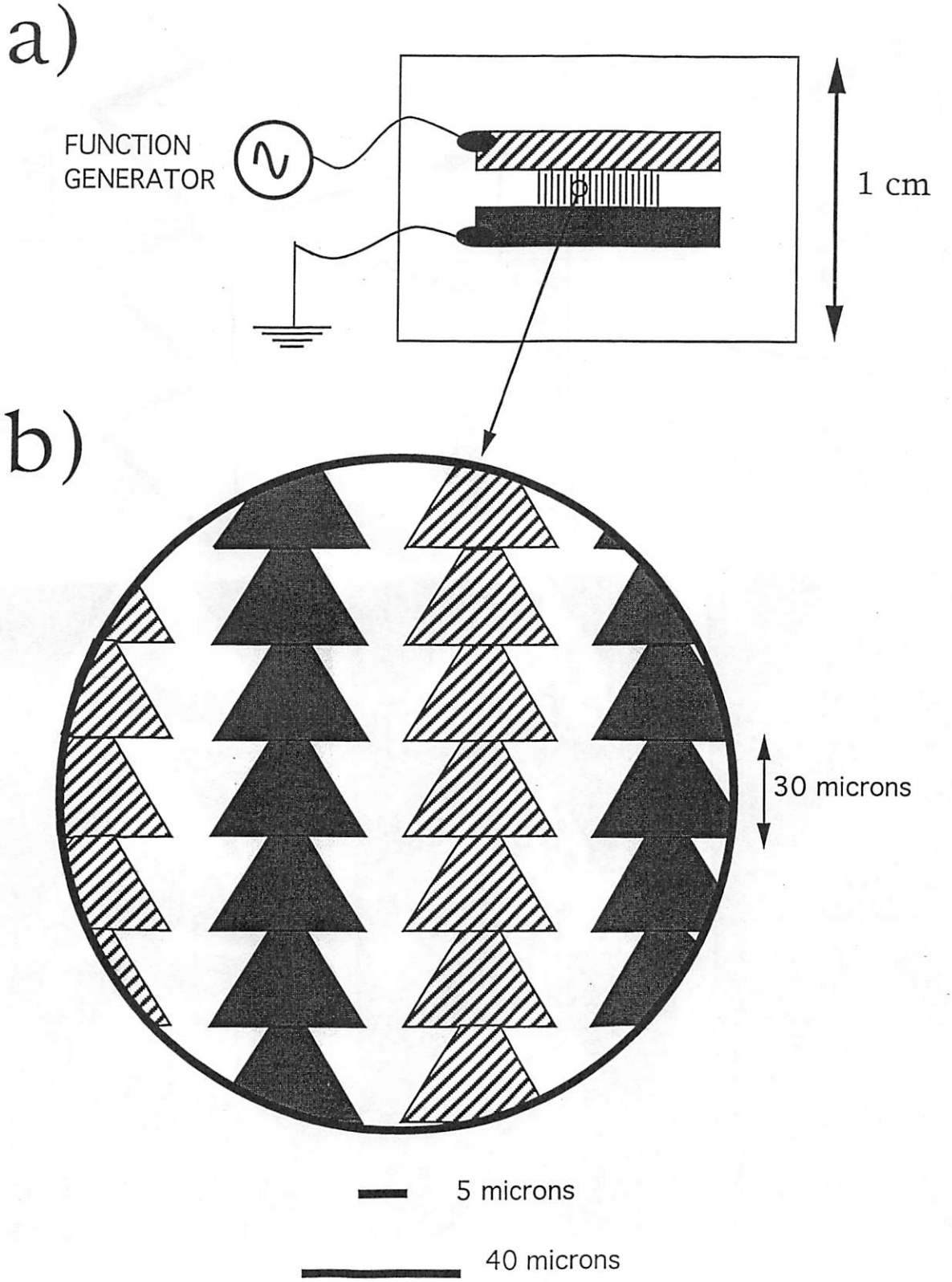

Faucheux and Libchaber
figure 2

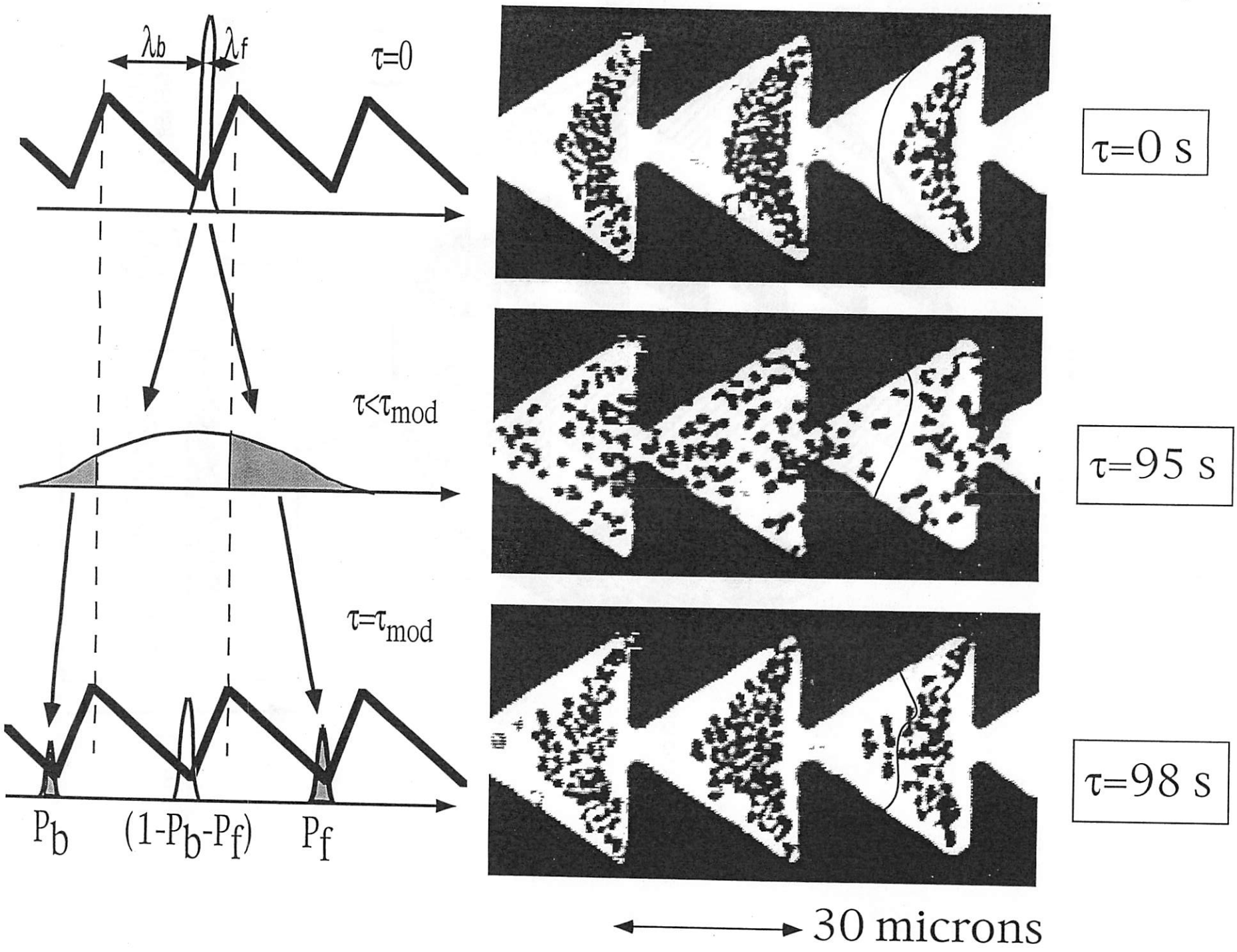

Faudeux and Libchaber

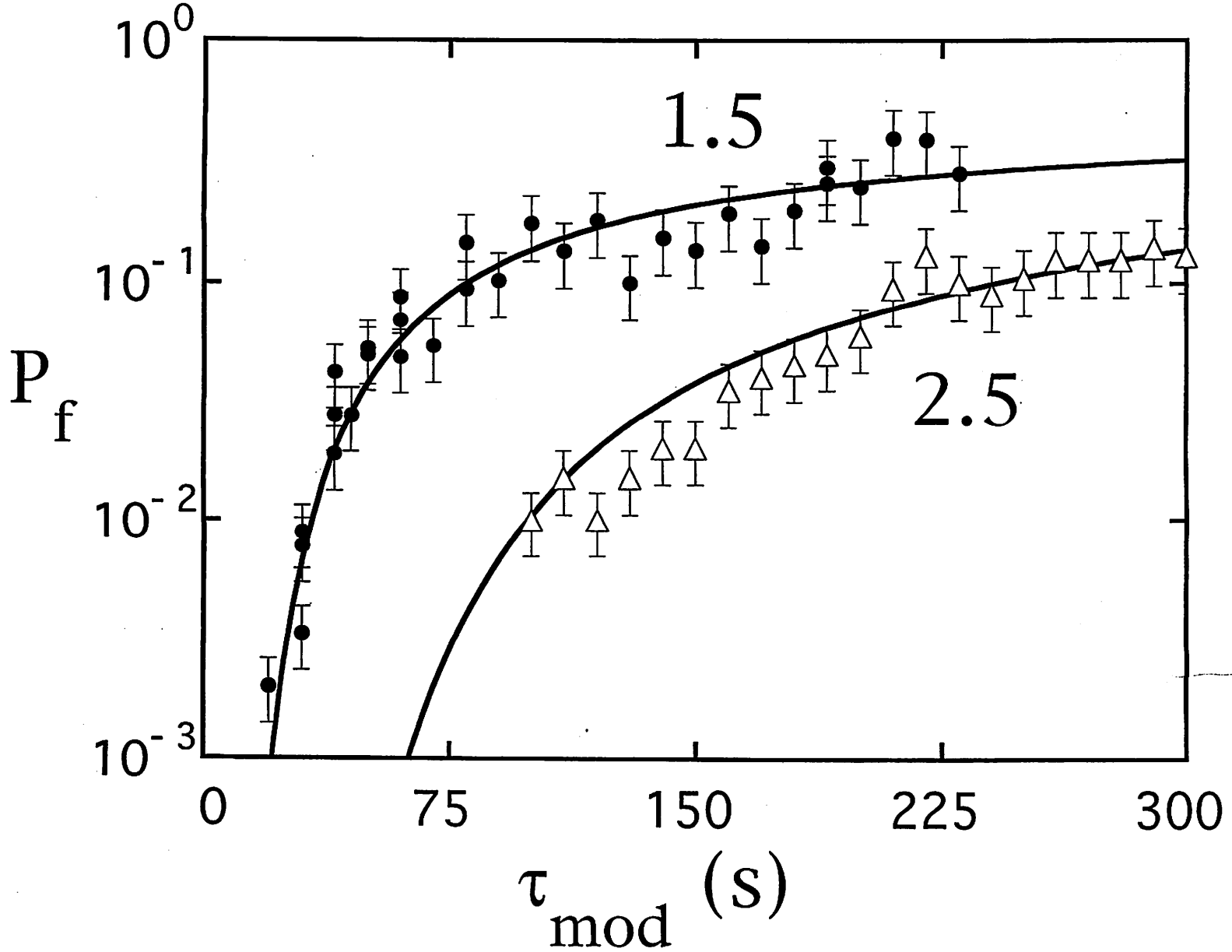

Faucheux and Libchaber

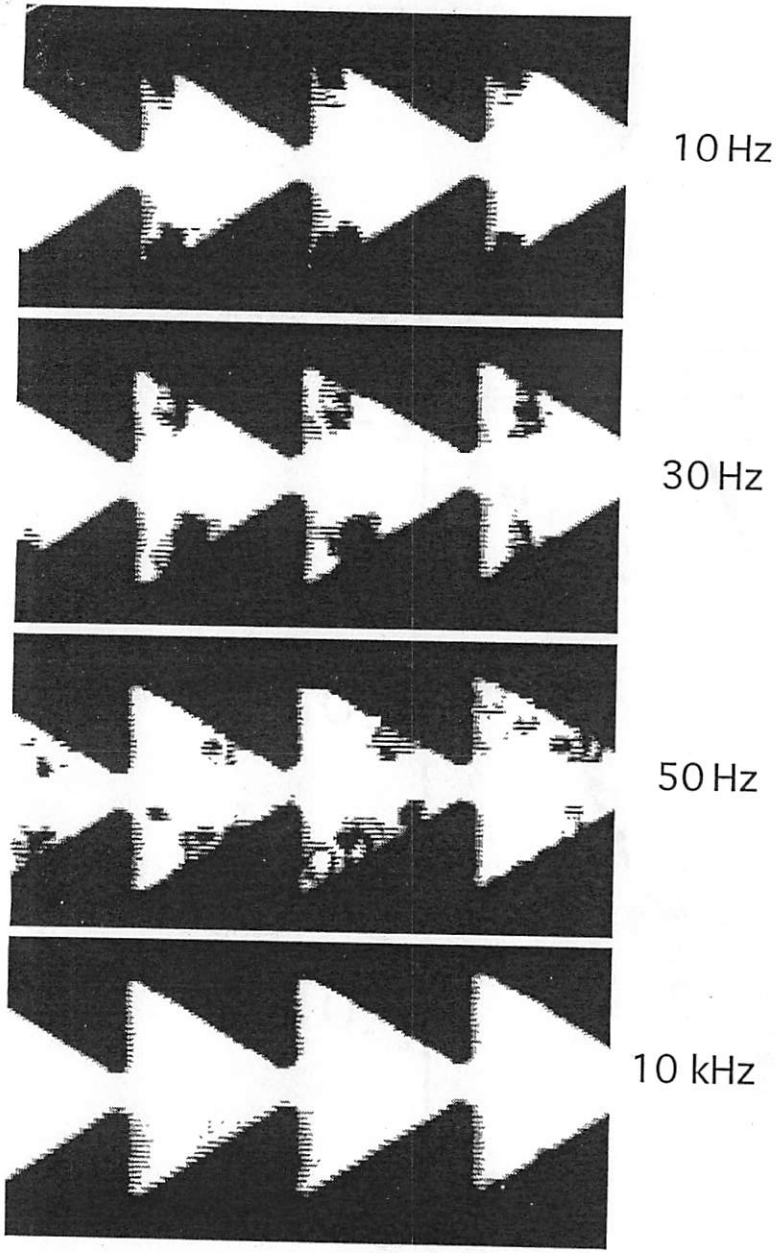

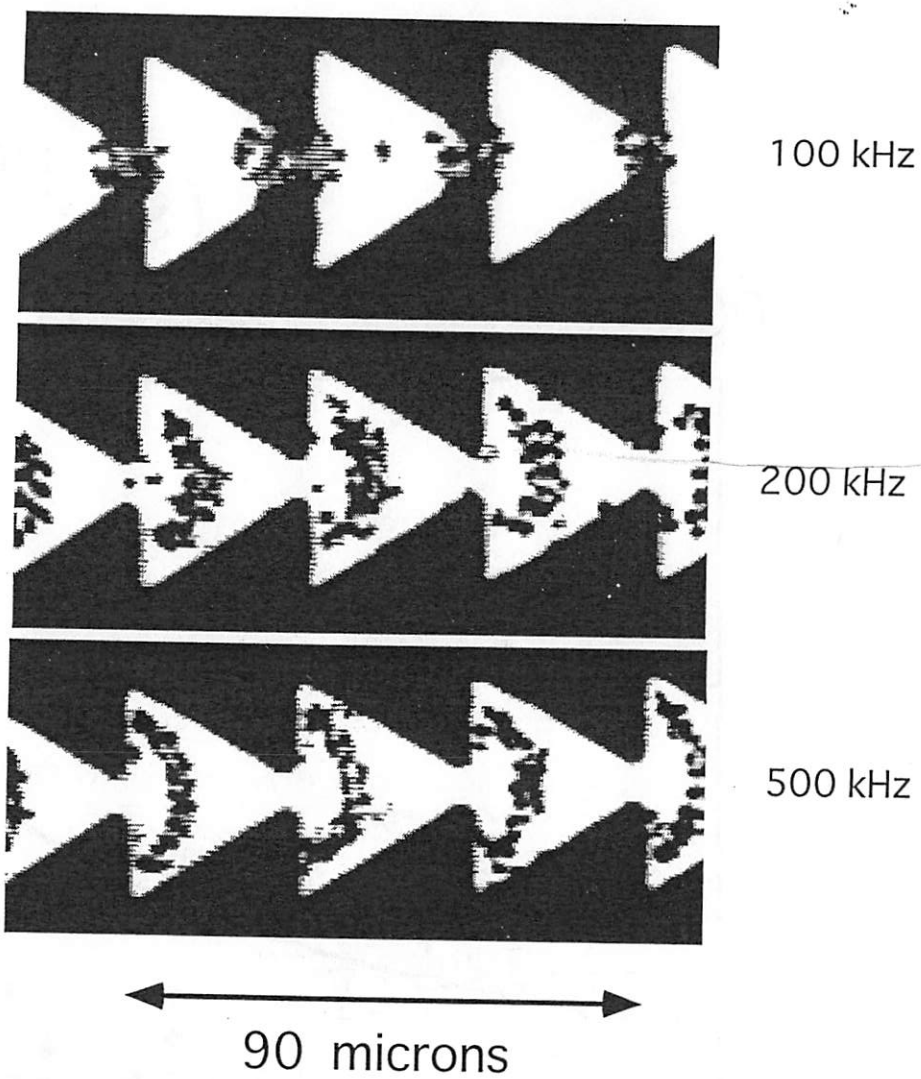

Faucheux and Libchaber
Fig 5